Russian Academy of Sciences
Joint Institute for High Temperatures RAS
Institute of Problems of Chemical Physics RAS
Kabardino-Balkarian State University

Physics of Extreme States of Matter — 2014

Moscow, 2014

Physics of Extreme States of Matter — 2014

Edited by academician Fortov V. E., Karamurzov B. S., Efremov V. P., Khishchenko K. V., Sultanov V. G., Levashov P. R., Andreev N. E., Kanel G. I., Iosilevskiy I. L., Mintsev V. B., Petrov O. F., Savintsev A. P., Shakhray D. V., Shpatakovskaya G. V.

This compendium is devoted to investigations in the fields of thermal physics of extreme states of matter and physics of high energy densities. Different models and results of theoretical calculations of equations of state for materials at high pressures and temperatures, physics of shock, detonation and combustion waves, interaction of intense laser, x-ray and microwave radiation, powerful particle beams with matter, techniques of intense energy fluxes generation, experimental methods of diagnostics of ultrafast processes, low-temperature plasma physics, issues of physics and power engineering, as well as technology projects are considered. The majority of the works has been presented at the XXIX International Conference on Equations of State for Matter (March 1–6, 2014, Elbrus, Kabardino-Balkaria, Russia). The edition is intended for specialists in physical and technical problems of power engineering.

This conference is dedicated to the centenary of birth of academician Yakov Borisovich Zel'dovich (March 8, 1914–December 2, 1987).

The conference is sponsored by the Russian Academy of Sciences and the Russian Foundation for Basic Research (grant No. 13-02-06212).

The editorial board announces with deep regret the death of the colleagues and friends, Dr. Vladimir Vladimirovich Milyavskiy (July 22, 1969–June 12, 2013), who was the organizing and program committees member of the Conferences on Equations of State for Matter and Interaction of Intense Energy Fluxes with Matter, and Prof. Gennady Vasil'evich Sin'ko (February 7, 1950–September 8, 2013), who was a regular and active participant of these conferences starting with one of the first meeting.

ISBN 978-5-94691-625-7

CONTENTS

CHAPTER 1. EQUATIONS OF STATE FOR MATTER

CHAPTER 2. SHOCK WAVES. DETONATION. COMBUSTION

CHAPTER 3. POWER INTERACTION WITH MATTER

CHAPTER 4. PHYSICS OF LOW TEMPERATURE PLASMA

TWO-TEMPERATURE EQUATIONS OF STATE FOR D-BAND METALS IRRADIATED BY FEMOTOSECOND LASER PULSES

***Migdal K. P.*[1] *, *Petrov Yu. V.*[2], *Zhakhovsky V. V.*[1], , *Inagamov N. A.*[2]**

[1] *VNIA, Moscow,* [2] *ITP RAS, Chernogolovka, Russia*

**migdal@vniia.ru*

The cold curves for energy and pressure of Copper, Iron, and Tantalum were obtained using methods of the density functional theory. Hydrostatic and uniaxial deformations in the range from double compression of the initial volume per atom to double stretching are considered. Allotropic transformation from α-phase of Iron to the hexaferrum with the growth of pressure is found at pressure of 13 GPa. We also obtained cold curves for two-temperature states in which crystal lattice at 0K and hot electrons are in the range from 1 kK to 55 kK. The behaviour of electronic internal energy, pressure, and density of states is investigated in the volume and temperature ranges mentioned above. The maximum hydrostatic strains and the types of lattice instabilities were theoretically predicted for the considered metals. At the first time the effecy of high electronic temperature on the electronic heat conductivity and electric resistivity is calculated for transition metals by the approach based on Boltzmann kinetic equation in τ-approximation.

Keywords: two-temperature state, phase transition in Iron, density functional theory, femtosecond laser

The femtosecond laser irradiation with optic wavelengths and moderate intensities acting on a metal surface is considered. With regard to metal the laser pulse energy is absorbed by free electrons on a depth of a skin layer. In this layer non-equilibrium energy distribution exists between electrons and ion lattice. In the present experimental data and theoretical calculations one have been demonstrated that a few picoseconds are required for electron-ion equilibration. The duration of electron-electron relaxation is order of magnitude 100 fs. We can consider surface layer as electron and ion subsystems, where the former obeys Fermi-Dirac distributions and has a temperature signifficantly greater than a temperature of the latter which is close to the metal initial temperature, $\sim$ 300K. This approach is valid in the case of the relation between two relaxation times mentioned above. During the two-temperature state (2T) a spatial distribution of atoms in lattice is constant because the electron-ion relaxation time is less than the typical time of acoustic unloading. Taking into account this circumstance we carried out the DFT calculation of electron thermodynamics properties for some metals in the wide range of electron temperatures and considered deformations. The similar volume and electronic temperature ranges have been considered in recent works [1, 2].

The influence of strong hydrostatic and uniaxial strains and compressions was investigated in the cold curve calculations for metals using DFT and taking into account probabilities of allotropic transformations.

Calculation method The cold curves of internal energies E and pressures P for metals with zero lattice temperature are obtained for Cu (fcc lattice), Fe (bcc and hcp), and Ta (bcc) in the range from double compression to double expansion using the DFT code VASP [3, 4]. We used PAW pseudopotentials with LDA and PBE forms of exchange-correlation functional. In the latter case the closest to the conduction bands for each metal p-electron band is additionally considered. Other used parameters: plane waves cutoff is 500 eV, 21^3 Monkhorst-Pack grid, and the number of free electron states is equal or greater than 20. These parameters were chosen as the result of convergence check and guarantee that convergence error is not greater than 1 %.

The validity of the value of expanded volume where metal lattice becomes unstable was approved by the DFT calculation of elastic moduli. The cutoffs were enlarged up to 600 eV (Cu), 800 eV (Fe), 650 eV (Ta). The obtained values for elastic moduli for some metal speciffic volumes at hydrostatic expansion allow to determine the type of lattice instability which is the reason of metal breakdown. The presence of hot electrons have been took into account with the use of smearing value and the Fermi-Dirac smearing was used. We carried out the calculation of 2T equations of state in the range from double compression to double expansion for electron temperatures up to 55 000K.

The results and comparison with experimental data. On the Fig. 1a the obtained cold curve for Cu is compared with the data of experiments [7, 8] in the case of compression. As we can see all curves are close to each other and the PBEpv curve is in better agreement with experimental data than other curves. The PBEpv curve for hcp (solid line) and bcc Fe (dashed line) is compared with the experimental data [13] obtained by ramp wave compression (RWC) method. This method allow to obtain the values of pressure for solid matter which cannot be achieved using previously used technique. In [13] the new record for solid Fe was received—560 GPa. It is necessary to notice that the dependence of pressure from compression obtained in this work not pure experimental curve but the result of experemental data treatment with the help of QMD simulation and Debye model. The analogous comparison for Ta is shown in Fig 1a where the experimental and FP-LMTO calculation data are in good agrement with our results (mainly PBEpv curve).

The dependences of Gibbs energy from pressure for bcc and hcp lattices of Fe are shown on the Fig 2a in the range of $\alpha - \epsilon$ allotropic transformation search. As the result of this search the pressure of bcc-hcp trans-

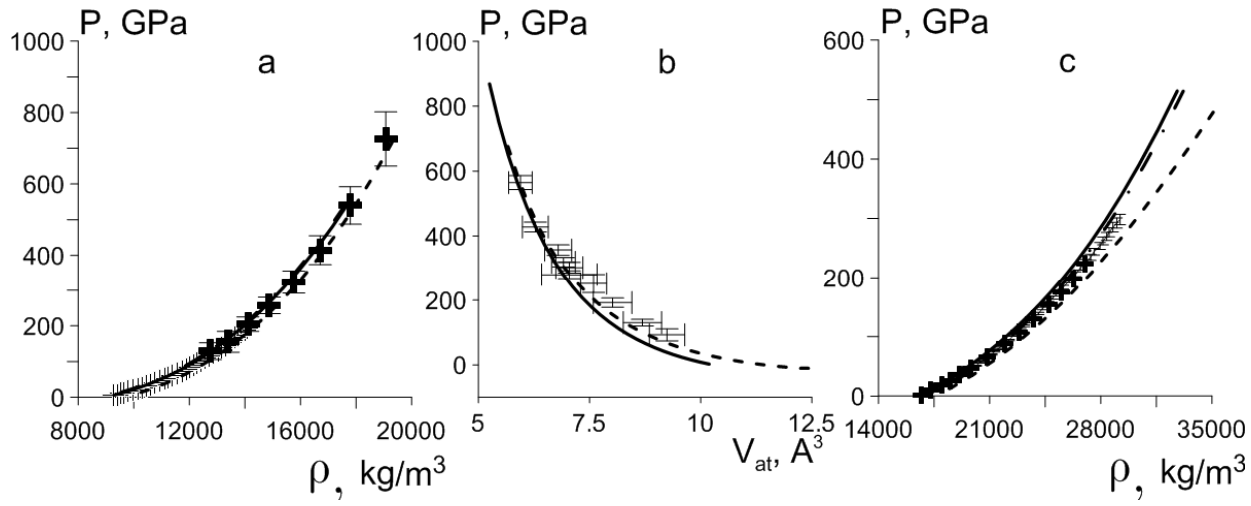

Figure 1. *Left panel.* The calculated pressure from density for compressed Cu using LDA (dash), PBE (dash-dot), and PBEpv (solid) pseudopotentials compared with the results of experiments [7] (open diamonds)[8] (thick crosses) *Middle panel.* The pressure from atomic volume for hcp (solid) and bcc (dash) compressed Fe calculated with the help of PBEpv pseudopotential and the result of recent ramp wave compression experiment [13] where anharmonic approximation for Debye-Waller factor calculation have been used. *Right panel.* The calculated pressure from density for compressed Ta using LDA (dash), PBE (dash-dot), and PBEpv (solid) pseudopotentials compared with the results of experiment [7] and FP-LMTO calculation [14] (thick crosses).

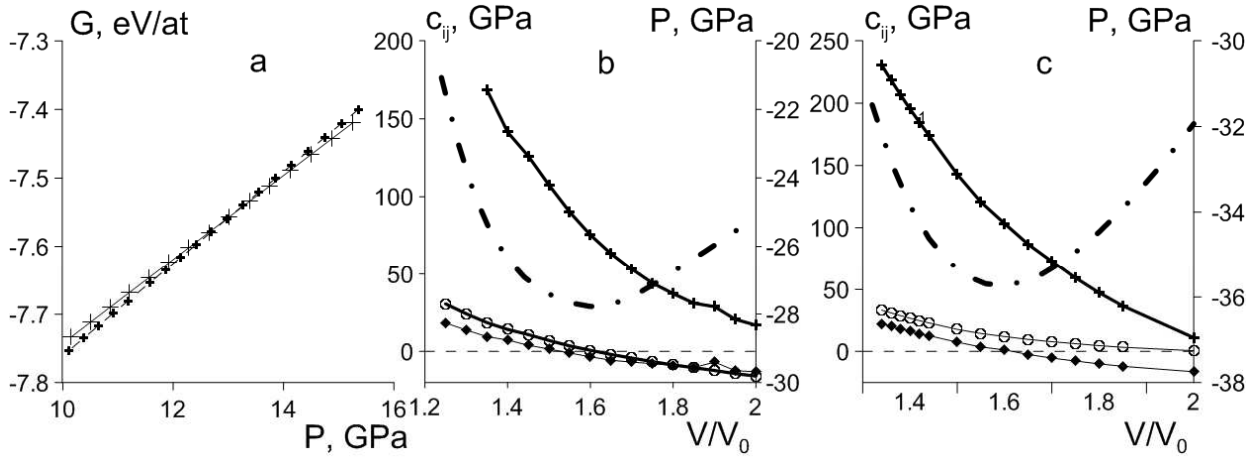

Figure 2. *Left panel.* The dependence of Gibbs energy from pressure for Fe in hcp (solid line, thin crosses) and bcc (dashed line, thick crosses) phases. *Middle panel.* Left Y scale: The dependence of elastic moduli combinations—criteria of lattice stability from relative specific volume in the case of Fe. The line with thick crosses corresponds to $c_{11} + 2c_{12}$ combination, open circles – $c_{11} - c_{12}$, diamonds – c_{44}. If the first combination is negative it means bulk instability, the second—shear instability, the third—tetragonal shear instability. Right Y scale: The dependence of pressure (dash-dot line) in bcc Fe from relative specific volume in the range corresponding to expansion. *Right panel.* The same values as in the middle panel for Ta.

formation is found with taking into account of uncertainties of G due to convergence error and finite step of the grid of pressure values. The found values is 14^{+5}_{-3} GPa (PBE) and 13^{+5}_{-2} (PBEpv) and in good agreement with the results of known experimental data [9]. This received values are obtained only after addition calculation on more denser gred (100 points of V/V_0 in the compression range from 0.9 to 1 V/V_0).

On the Fig 2b and 2c the values for Fe and Ta of elastic moduli combinations which negative values (even if one of them) determine the area of lattice instability in the case of hydrostatic expansion. The minimum value of pressure is achieved at the specific volume where the lattice becomes unstable. As we can see for both metals the results for cold curves and more accurate elastic moduli calculations are in good agreement because the growth of pressure with volume is obvious case of unphysical behaviour at expansion.

The results for 2T EoS for Cu, Fe, and Ta are shown on Fig 3 as the dependencies of pressure from density at some values of electron temperature. The influence of additionally considered p-electron band in PBE pseudopotential is negligible for most cases (cannot be shown on this figure) and only for strong compression of Ta (Fig 3c) the difference caused by this band is sufficient to take it into account. The positive shift

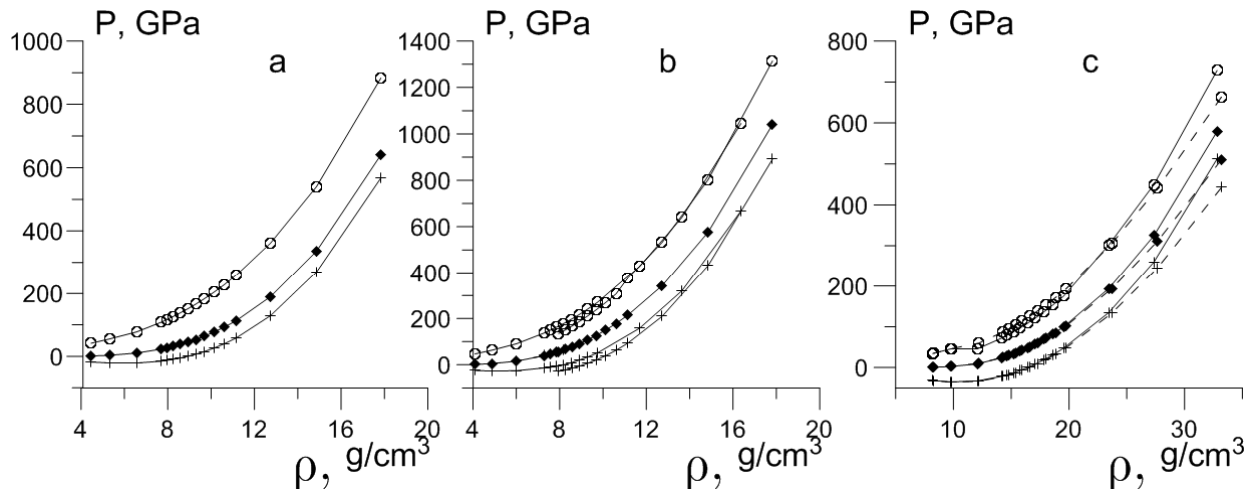

Figure 3. The dependence of pressure from density at hydrostatic deformations obtained with the use of PBEpv pseudopotential for fixed values of electron temperature T_e=1000 K (thin crosses), 25000 K(diamonds), 55000 R (open circles). *Left panel.* The case of Cu. *Middle panel.* The case of bcc and hcp Fe. For the values of T_e 1000 K and 55 000 K the hcp curves is always low than bcc. For the value of T_e the difference between two curves are negligbly small. *Right panel.* The case of Ta. The dashed lines corresponds to dependences obtained with the use of PBE pseudopotential.

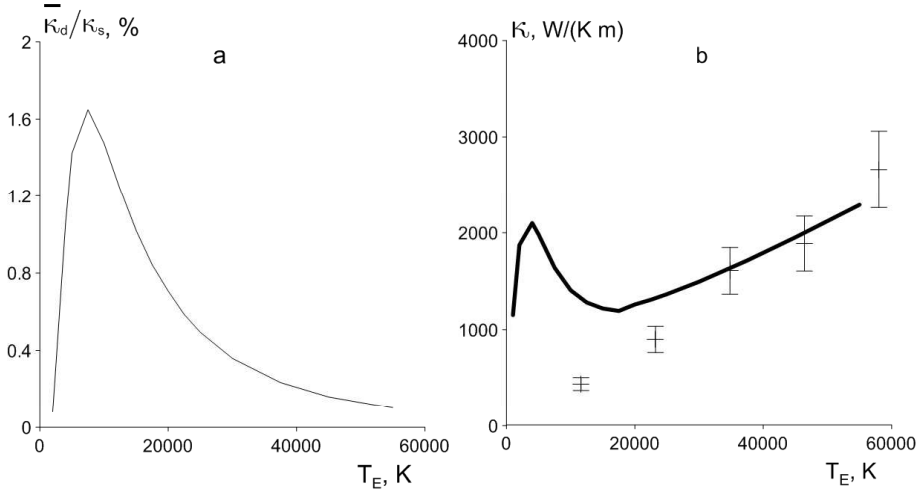

Figure 4. *Left panel.* The dependence from electron temperature of the overestimated d-electron thermal conductivity divided by s-electron thermal conductivity for Cu. *Right panel.* The dependence from electron temperature of the s-electron thermal conductivity for Au and quantum molecular dynamics simulation performed in [6].

of pressure due to the growth of electron temperature is more noticeable for Cu than for transition metals. In the case of Fe the described above bcc-hcp transition cannot be reliably found at the demonstrated values for electron temperature 25000K and 55000K. We can explain such behavior of Fe as the consequence of decrease of lattice ifluence on metal state when the electron subsystem energy becomes sufficiently high.

Electronic transport coefficients calculation. The calculation of the electron conductivity coefficient was carried out with the use of approach [5, 10] which is based on the result for Boltzmann kinetic equation for free electrons in the relaxation time approximation. On Fig 4a the data for κ_{2T} obtained with taking into account of the electronic spectra dependence from electron temperature and found previously [10] are represented. Even if we neglect the frequency of d-electron – ion collisions so the result for d-electron conductivity $\kappa_{2T,d}$ is overestimated, the value of $\frac{\kappa_{2T,d}}{\kappa_{2T,s}}$ is less than 0.02 on the full electron temperature range. The calculated by DFT partial electron densities of states allow us to check the statement that the s-electron impact in electronic conductivity is dominated. On Fig 4b the comparison between the results for κ_{2T} obtained in our two parabolic approximation [10] and QMD calculations based on Kubo-Greenwood approach [6] is provided for the case of Au. We can see on Fig 3a that two areas of electron temperatures exist. On the first area where $T_e < 30000$K our result has a peak at 5000 K and slightly decrease while the QMD values increase monotonously with T_e. The second area starts from $T_e > 30000$K and there the considered results are in good agreement. Authors supposed that the peak of κ_{2T} is the consequence of weak d-band influence on

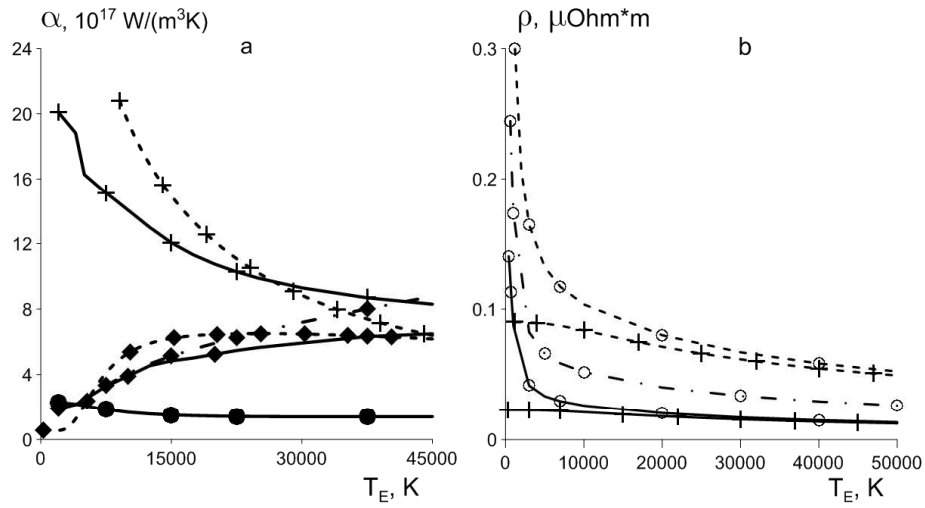

Figure 5. *Left panel.* The dependence from electron temperature of electron-ion coupling for Cu (diamonds), Fe (thick crosses) and Ta (open crosses). The obtained with taking into account of $g(T_e)$ dependence data for Cu and Fe ars shown by solid lines. The previous result for Cu without the consideration of electron temperature influence on DOS is shown by dash-dotted line and the results from web resource [15] are shown by dashed line. *Right panel.* Resistivities σ of Au (thick crosses) and Ni (open circles) as function of electron temperature T_e. The functions $\sigma\mathrm{Au}(T_e)$ are given at two fixed values of lattice temperature (300 K—solid line, 1200—dashed line) and $\sigma_{\mathrm{Fe}}(T_e)$ at the fixed ion temperatures T_e=300 K (solid), 600 K (dash-solid) and 1200 K (dash)

collision frequencies at temperatures which less than the absolute value of d-band edge $\epsilon_{2,Au} = -1.7$eV.

Taking into consideration the electron temperature influence on electron density of states causes the noticeable decrease of electron-ion coupling in the case of Cu, as we can see on Fig 5a. The represented on Fig 5a values of coupling a was obtained using Kaganov-Lifshitz-Tanatarov approach [10, 11].

Also the contribution of electron-phonon interaction in energy and charge transfer was carried out at high electron temperatures. The determination of this contribution makes possible to obtain the accurate analytical expression for electron resistivity of metal with hot electrons [12].

The phonon spectra was approximated by modified Debye approach where the deviation from linear acoustic behavior at large values of phonon momentum is taking into account. For two-band metals all possible processes for s- and d-band electrons are considered and the conditions on the values of electron and phonon momenta have been taken into account during Boltzmann kinetic equation solutions integration. These solutions were obtained for electrons interacting with outer electric field in relaxation time approximation. The electric conductivity is determined with the use of Ohm law.

As a result the curves of electric conductivity σ dependence from T_e was calculated fro Au and Ni. On the Fig 5b one demonstrated that the value σ is almost not depend from T_e for noble metals(Au). But the same value for Ni demonstrates steep decreasing at temperatures is order of magnitude of melting temperature for Ni. It is worth to notice that the demonstrated dependence was not taking into account in the previous known to the authors works.

This work was supported by RFBR (grant No 13-02-1078).

1. Khakshouri S., Alfé D, and Duffy D. M., // Phys. Rev. B. 2008. V. 78. P. 224304.
2. Sin'ko G. V., Smirnov N. A., Ovechkin A. A., Levashov P. R., Khishchenko K. V., // HEDP. 2013. V. 9. No. 2. P. 309.
3. Kresse G., Furthmuller J., // Comput. Matter. Sci. 1996. V. 6. No. 1. P. 15.
4. Kresse G., Furthmuller J., // Phys. Rev. B. 1996. V. 54. P. 11169.
5. Inogamov N. A., Petrov Yu. V., // JETP. 2010. V. 110. No. 3. P. 446.
6. Norman G., Saitov I., Stegailov V., Zhilyaev P., // Contrib. to Plasma Phys. 2013. V. 53. No. 4-5. P. 300.
7. Chijioke A. D., Nellis W. J., Silvera I. F. // Journal of Applied Physics. 2005. V. 98. P. 073526.
8. Dewaele A., Loubeyre P. Mezouar M. // Phys. Rev. B. 2004. V. 70. P. 094112.
9. Wang F. M., Ingalls R. // Phys. Rev. B. 1998. V. 57. No. 10. P. 5647.
10. Petrov Yu. V, Inogamov N. A., Migdal K. P. // JETP Letters. 2013. V. 97. No. 1. P. 20.
11. Kaganov M. I., Ligshits I. M., Tanatarov L. V. // Sov. Phys. JETP. 1956. V. 4. No. 173.
12. Migdal K. P., Petrov Yu. V., Inogamov N. A. // Proc. of SPIE. 2014. in press.
13. Ping Y., Coppari F., Hicks D.Ǵ. et al // Phys. Rev. Lett. 2013. V. 111. P. 065501.
14. Cynn H., Yoo C.-S. // Phys. Rev. B. 1999. V. 59. P. 8526.
15. faculty.virginia.edu/CompMat.